

# Ten Milliparsec-Scale Structure of the Nucleus Region in Centaurus A

Shinji HORIUCHI,<sup>1</sup> David L. MEIER,<sup>2</sup> Robert A. PRESTON,<sup>2</sup> and Steven J. TINGAY<sup>1</sup>

<sup>1</sup>*Centre for Astrophysics and Supercomputing, Swinburne University of Technology,  
Mail No. H39, PO Box 218, Hawthorn, Victoria 3122, Australia  
shoriuchi@swin.edu.au*

<sup>2</sup>*Jet Propulsion Laboratory, Mail Code 238-322, California Institute of Technology,  
4800 Oak Grove Drive, Pasadena, CA 91109, USA*

(Received 2005 July 11; accepted 2005 August 16)

## Abstract

We present the results of a VLBI Space Observatory Programme (VSOP) observation of the subparsec structure in Cen A at 4.9 GHz. The observation produced an image of the subparsec jet components with a resolution of three-times better than images from previous VLBI monitoring campaigns at 8.4 GHz, and twice better than the previous 22 GHz studies. Owing to its proximity, our Cen A space-VLBI image is one of the highest spatial-resolution images of an AGN ever made — 0.01 pc per beam — comparable only to the recent 43 GHz VLBI images of M 87. The elongated core region is resolved into several components of over 10 milliarcsec long (0.2 pc), including a compact component of brightness temperature  $2.2 \times 10^{10}$  K. A counterjet was detected: if we assume jet-counterjet symmetry, a relatively slow jet speed, and a large viewing angle, as derived from previous observations, the image allows us to investigate the distribution of ionized gas around the core, which is opaque at this frequency due to free-free absorption. We also analyzed the jet geometry in terms of collimation. Assuming the strongest component to be the core, the jet opening angle at  $\sim 5000 r_S$  from the core is estimated to be  $\sim 12^\circ$ , with the collimation of the jet to  $\sim 3^\circ$  continuing out to  $\sim 20000 r_S$ . This result is consistent with previous studies of the jet in M 87, which favor MHD disk outflow models. Future space VLBI observations at higher frequencies will probably be able to image the collimation region, within  $1000 r_S$  of the center of Cen A, together with the accretion disk itself.

**Key words:** galaxies: active — galaxies: individual (Centaurus A) — techniques: interferometric

## 1. Introduction

Centaurus A (NGC 5128) is the closest radio galaxy, at a distant of only 3.4 Mpc (Israel 1998). This proximity allows higher resolution imaging than that obtained for more distant galaxies, resulting in Cen A being one of the most important targets for the study of jet formation and collimation mechanisms in active galactic nuclei (AGNs). The estimated mass of the central black hole, based on infrared observations of a 20 pc central disk, is  $2.0_{-1.4}^{+3.0} \times 10^8 M_\odot$  (Marconi et al. 2001). Observations with VLBI arrays can obtain images of the nuclear radio source in this galaxy with a linear resolution of 0.02 pc ( $\sim 1000 r_S$ ) for a 1 mas angular resolution.

Previous VLBI monitoring of Cen A shows that the subparsec-scale jet has components with a slow proper motion away from the nucleus of approximately  $0.1 c$ , while irregular episodes of rapid evolution within the jet component suggest that the underlying flow of the jet is much faster, and probably greater than  $0.45 c$  (Tingay et al. 1998, 2001). Considering the likely jet speed and the jet-to-counterjet surface brightness ratio (Jones et al. 1996), Tingay et al. (1998) concluded that the subparsec-scale jet is inclined to our line of sight by between  $50^\circ$  and  $80^\circ$ . These results are in contrast with a recent analysis based on the VLA observations for 100 pc scale jet, which suggests apparent subluminal motions of approximately  $0.5 c$  and a significantly smaller angle to the line of sight of  $\sim 15^\circ$  (Hardcastle et al. 2003). Using the VLBA at 43 GHz, Kellermann, Zensus, and Cohen (1997) measured the

size of the compact radio nucleus of Cen A to be about 0.5 mas (0.01 pc) by fitting the visibilities with a circular Gaussian component. However, the coverage of the  $(u, v)$ -plane with the VLBA alone is severely limited because the source is so far south, and they were unable to construct an image of the nucleus.

To study the nature of the nuclear region, we conducted a space VLBI (VSOP) monitoring program of Cen A, observing with the HALCA space telescope (Hirabayashi et al. 1998) at 4.9 GHz and 1.6 GHz, from mid-1999 to mid-2000 when the  $(u, v)$ -coverage was optimal (Horiuchi et al. 2002). Space-ground baseline fringes of Cen A were detected for the first time, although the signal-to-noise ratio became rapidly smaller as the space baseline length became larger than one Earth's diameter. These observations produced images of the subparsec jet components with a resolution of several-times better than images in an ongoing 8.4 GHz monitoring campaign and a few times better than 22 GHz studies.

In this paper we highlight the highest quality image obtained from an observation on 2000 August 6, due to sensitive telescopes, especially the phased VLA and ATCA, which joined the ground telescope array. Owing to its proximity, our Cen A space-VLBI images are some of the highest spatial resolution images ever made of an AGN — 0.01 pc per beam — comparable only to the 43 GHz VLBI images of M 87 (Junor et al. 1999). We discuss the structure of the core region and the implications of the remarkably collinear jet extending from the core region to the 1 pc scale.

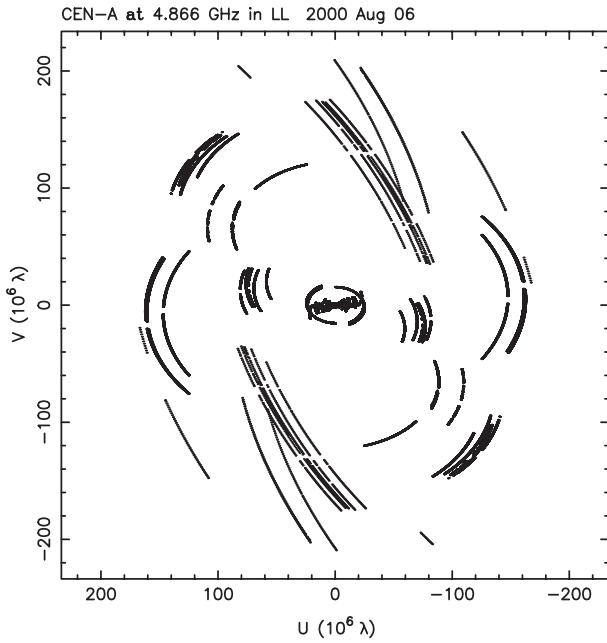


**Fig. 1.** The  $(u, v)$ -coverage of the VSOP observation. The solid lines are for the ground baselines and the dotted lines (the long, straight diagonal tracks) are space baselines where fringe-fitting was successful.

## 2. Observations and Results

The observations presented here were conducted as a part of the VSOP observation series to monitor the evolution of Cen A over 18 months, starting on 1999 January, mainly at 4.9 GHz. The observing frequency was at 4.866 GHz for a 16 MHz bandwidth with 2-bit sampling. The observation was divided into two parts for different correlators. From 2000 August 6 21:00 UT to August 7 02:30 UT, the participating ground telescopes were six of the 10 VLBA stations (FD, KP, LA, MK, OV, PT), the VLA and ATCA (Narrabri), with the data correlated at the Socorro VLBA correlator. From August 7 03:00 UT to 13:00 UT, the ground telescopes were the ATCA, Ceduna, Mopra, Hartebeesthoek, and VLBA-Mauna Kea, with the data correlated at the Penticton S2 correlator. The space data obtained with the HALCA satellite was downloaded and recorded in the VLBA format at the Green Bank tracking station for the first part of the observation, and in the S2 format at the Madrid, Tidbinbilla, and Goldstone stations for the latter part.

The data from the correlators were exported into the Astronomical Image Processing System (AIPS) as FITS files, amplitude calibrated, fringe-fitted, and averaged before standard VLBI imaging procedures in Difmap. The source was highly resolved on the longer baselines, and fringe-fitting for HALCA was only successful for projected baselines up to an Earth's diameter. This was consistent with the previous VSOP series on this source (Fujisawa et al. 2000) in which no space fringes were detected. The  $(u, v)$ -coverage of the data used for imaging is shown in figure 1. An image obtained from this  $(u, v)$ -coverage is shown in figure 2. The rms noise level of the space VLBI image is  $0.90 \text{ mJy beam}^{-1}$  for the peak level

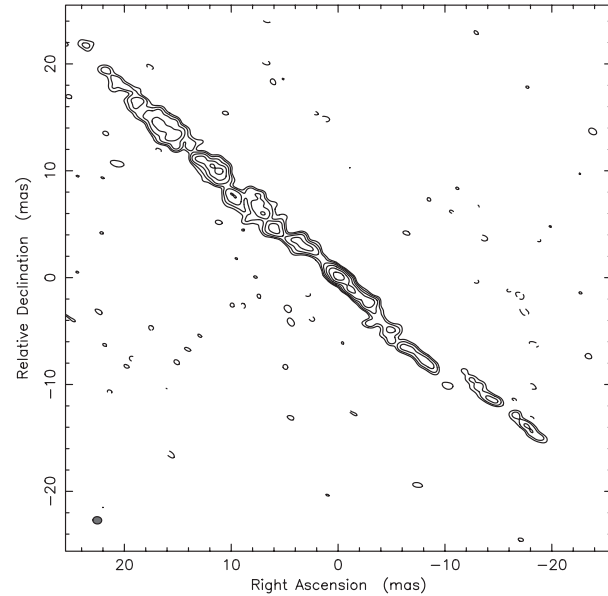


**Fig. 2.** Full resolution VSOP image of the inner 40 mas around the peak. The FWHM of the restored beam is  $0.827 \times 0.68 \text{ mas}$  at a PA of  $86^\circ 2$ , as indicated in the small filled circle at the bottom left-hand corner. Contours are drawn at  $-2, 2, 4, 8, 16, 32,$  and  $64\%$  of  $0.182 \text{ Jy beam}^{-1}$ , the peak flux density in the map.

of  $182 \text{ mJy beam}^{-1}$ , corresponding to a dynamic range of 200. An image obtained from the ground baselines only (solid lines in figure 1) is shown in figure 3. This image yields an rms noise level of  $0.57 \text{ mJy beam}^{-1}$  and a peak level of  $167 \text{ mJy beam}^{-1}$ , and hence a dynamic range of 293.

In both images the jet is remarkably linear and oriented along a position angle of  $\sim 51^\circ$  with several components visible. The brightest part of the jet has an elongation northeast and a counterjet to the southwest. It is not easy to distinguish between the core and the jet with a single epoch, single frequency map for such a complicated source. The nucleus region of Cen A is substantially affected by both synchrotron self-absorption and free-free absorption, which are both frequency-dependent effects. Tingay and Murphy (2001) registered images of 2.2 GHz, 5.0 GHz, and 8.4 GHz restored using an average restoring beam of  $19 \times 6 \text{ mas}$  at a position angle of  $4^\circ$ , in order to estimate the free-free optical depth and the intrinsic spectral index. They found that the core has a comparable flux to the jet at 5 GHz, while the core dominates the jet at 8 GHz and the core is substantially absorbed and invisible at 2.2 GHz. To identify the core region we compared Tingay and Murphy's 5.0 GHz VLBA image at 1999 May 4 (figure 4-a) and our image (figure 4-b), both restored with the same beam as originally used by Tingay and Murphy (2001). In spite of the 15 month separation between these two observations, the images appear to be very similar at this resolution; hence, we concluded that the brightest part around the phase center in our image corresponds to the core region, in which the 2.2 GHz flux would be substantially absorbed, as observed by Tingay and Murphy (2001).

The surface brightness of both the original image (figure 3)

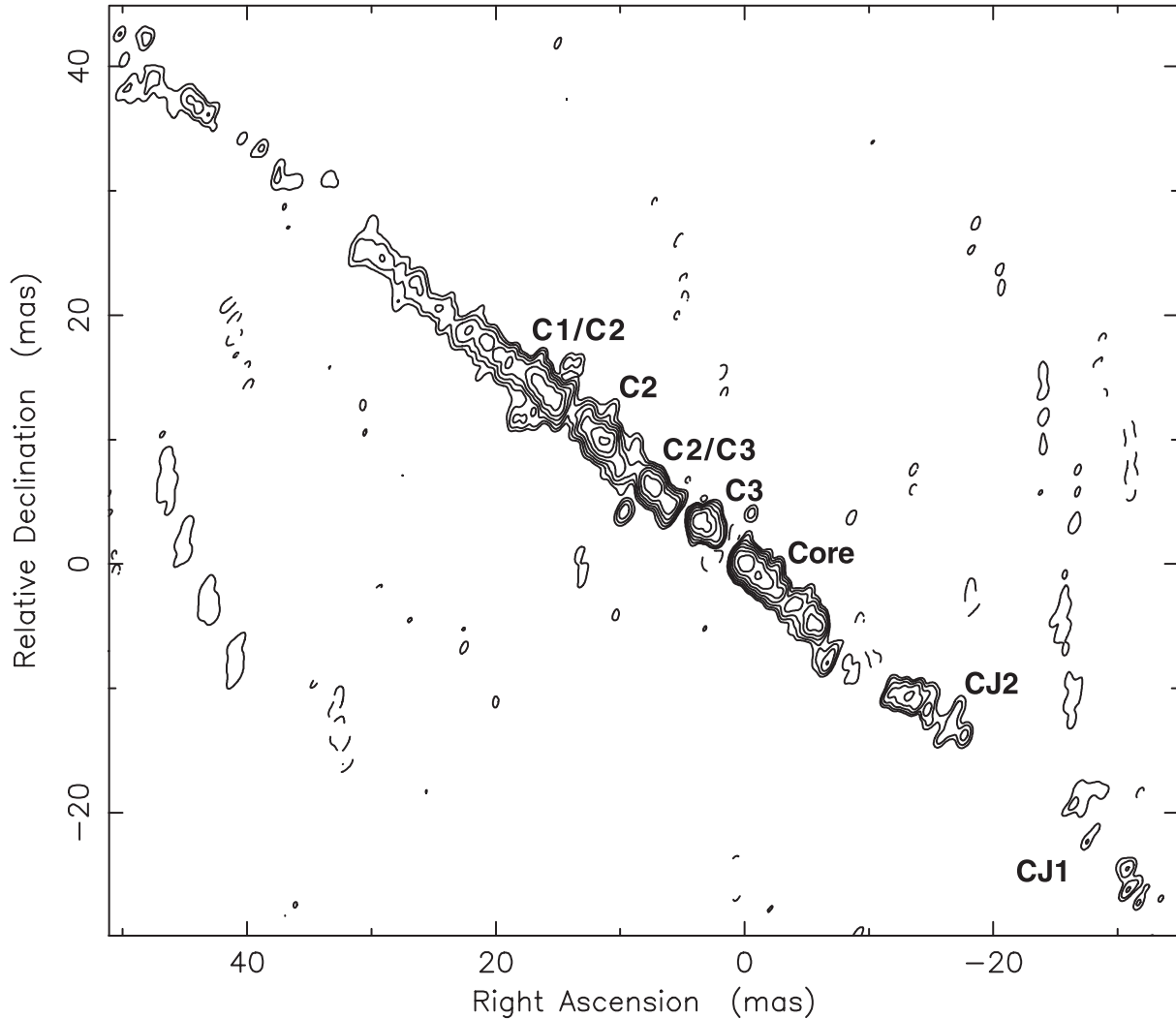


**Fig. 3.** Image obtained from only the ground telescopes. The FWHM of the restored beam is  $1.19 \times 0.61$  mas at a PA of  $-27^\circ 5$ . Contours are drawn at  $-0.8, 0.8, 1.6, 3.2, 6.4, 12.8, 25.6,$  and  $51.2\%$  of  $0.167 \text{ Jy beam}^{-1}$ , the peak flux density in the map.

and the lower resolution image (figure 4-b) is illustrated in figure 5 as a “slice” profile along the jet. Assuming that the elongated region that includes the brightest part is the core, the identification of large-scale components over 60 mas (C1, C2, C3, CJ1, and CJ2) was adopted from a comparison to the previous VLBI monitoring (Tingay et al. 1998, 2001). In our image there are 4 distinctive bright parts in the jet for C1, C2, and C3, which leave some ambiguity in the identification. Hence, we tentatively denote a component between possible C2 and C3 as “C2/C3”, and another component northeast of C2 as “C1/C2”. In previous VLBI monitoring (Tingay et al. 1998, 2001), both C1 and C2 showed elongated linear structures along the jet, and the fitted lengths were sometimes up to around 20 mas, depending on the observing epoch. It is likely that our observation resolves those two regions into more than two components.

Fujisawa et al. (2000) claimed to have found a large bending of a jet close to the position of component C3 from the VSOP observation at 5 GHz in 1998 January. Our observation had a much better  $(u, v)$ -coverage and twice better resolution

perpendicular to the jet: no such bending is recognizable in our image. However, because of  $-43^\circ$  declination of Cen A and the positional relation between the VLBA and the other southern hemisphere ground telescopes, our data still suffer large  $(u, v)$  holes over the intermediate resolution range of  $50\text{--}100 M\lambda$ , especially at position angles similar to the jet direction. To prove the reliability of our Cen A map, as shown in figure 3, we made a couple of tests: 1) We retained clean components for only the 5 brightest features, from the core region through the C1/C2 components in the map, and examined how well they alone fit the data. We observed that about 40% of the flux on the shortest baselines correspond to the residuals, while the visibilities on the longer baselines fit the model very well, indicating there is significant structure that is not accounted for in the simple map. Finally, we exported the retained clean components to the original  $(u, v)$  data before clean-selfcalibration iteration and confirmed that the residual map clearly showed weaker features, such as a counterjet. 2) We tried model-fitting for the visibility data and see how many components are definitely required before

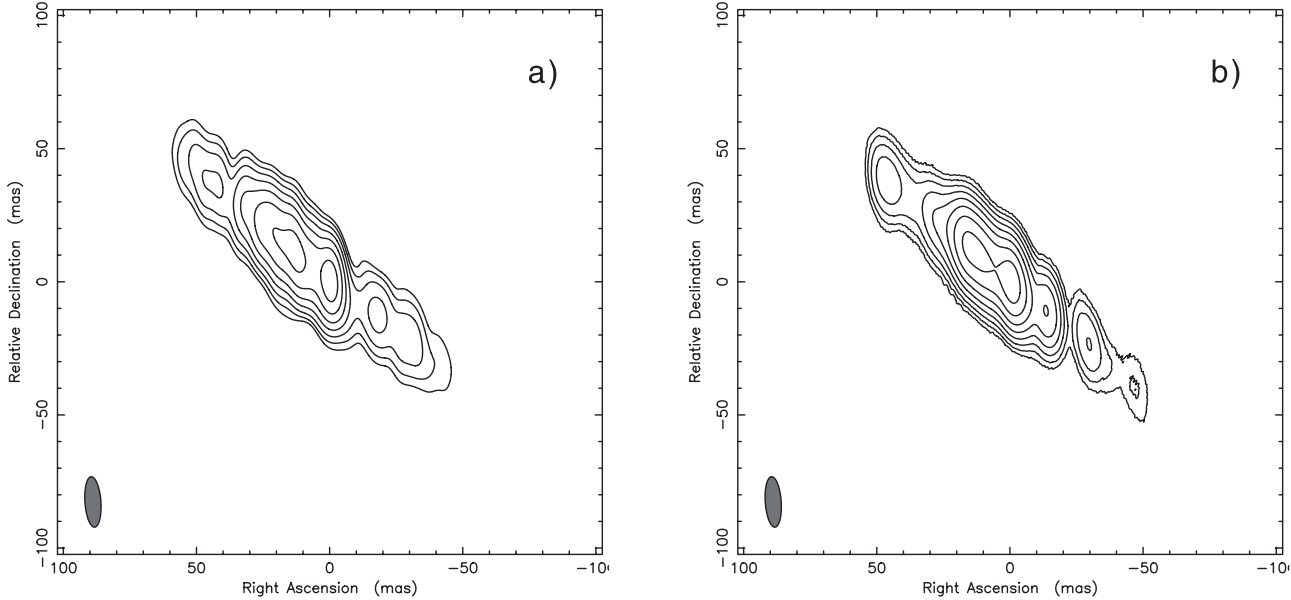


**Fig. 4.** (a) 5.0 GHz VLBA image at 1999 May 4 (Tingay, Murphy 2001). (b) Image from the same data for figure 3. Both images were restored with the larger beam of  $19 \times 6$  mas at a position angle of  $4^\circ$ , as used by Tingay and Murphy (2001) for spectral analysis. Contour levels are  $-1, 1, 2, 4, 8, 16, 32,$  and  $64\%$  of  $0.854 \text{ Jy beam}^{-1}$ , the peak flux density in the map, for (a), and  $-0.5, 0.5, 1, 2, 4, 8, 16, 32,$  and  $64\%$  of  $0.839 \text{ Jy beam}^{-1}$  for (b).

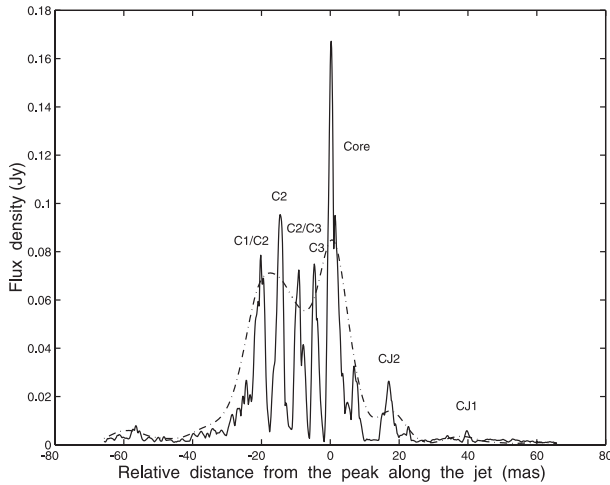


**Fig. 5.** Surface-brightness profile image along the PA  $51^\circ$  corresponding to the jet axis. The line represents the ground baseline image shown in figure 1, and the dotted line represents that convolved with the larger beam shown in figure 4, with the amplitude scaled to 0.1 times for comparison. The identifications of the components for the Core, C1, C2, C3, CJ1, and CJ2 are adopted from Tingay, Preston, and Jauncey (2001).

there is ambiguity as to what additional components (if any) should be added. We found up to 12 required components, whose positions are reasonably consistent with the features in the original map as shown in figure 3.

To quantify the structure of the nuclear region of Cen A, the image obtained using the array of ground telescopes only (figure 3) was analyzed using the AIPS task JMFIT to model fit each subcomponent with a Gaussian profile. This procedure is more reliable than fitting models to the  $(u, v)$  data when the high-resolution visibilities are too complex to fit the model

meaningfully. Table 1 gives the parameters obtained from the model fit. The brightest core feature around the phase center is modeled with 4 components labeled with Core1, Core2, Core3, and Core4. The brightness temperature,  $T_b$ , is also derived for each component, and listed in table 1.

### 3. Discussion

#### 3.1. Identification of the Core and the Brightness Temperature

We resolved the core region into several components. We also successfully detected a few components of the counterjet. As we described earlier, it is difficult to identify the core itself from only one epoch at a single frequency. This is especially the case if we have no other images to compare at similar resolution. If the jet and the counterjet are intrinsically symmetric and ejected from the core symmetrically, we should be able to know the location of the core as the origin of both the jet and counterjet. Under the simple beaming model for a symmetric jet system with an equal and constant bulk and pattern speed, the ratio of the apparent distances from the core of equivalent components in the approaching and receding jets, in terms of the bulk velocity of material in the jet ( $\beta = v/c$ ) and the angle to the line of sight  $\theta$ , is  $D = (1 + \beta \cos \theta)/(1 - \beta \cos \theta) \sim 1.1$  for the typical values of  $v \sim 0.1 c$  and  $\theta \sim 60^\circ$  adopted from the monitoring results of Tingay et al. (1998) and Tingay, Preston, and Jauncey (2001) for the jet components C1 and C2. This gives an upper limit of displacement of the core from the apparent geometrical center, which is only applicable for the outer jet components, such as C1 and C2, and there would be no such displacement expected for inner components such as C3 since no significant motion has been recognized in the monitoring. The derived mild upper limit of  $D$  for Cen A is in contrast with other radio source



**Table 1.** Models for the image shown in figure 3.

Flux (Jy)	Radius (mas)	$\theta$ (deg)	Major axis (mas)	Axial ratio	$\psi$ (deg)	$T_b$ $10^{10}$ K	ID
0.478	0.00	0.00	1.52	0.49	50.6	2.19	Core1
0.235	1.98	-139.1	2.76	0.17	53.5	0.91	Core2
0.370	4.96	-141.5	2.13	0.62	80.7	0.68	Core3
0.121	7.14	-139.0	1.75	0.63	47.6	0.32	Core4
0.274	5.10	45.0	1.84	0.58	61.3	0.72	C3
0.326	9.39	49.3	2.59	0.32	45.9	0.78	C2/C3?
0.416	15.11	48.5	2.10	0.45	45.4	1.09	C2
0.403	20.79	49.1	2.44	0.45	44.0	0.78	C1/C2?
0.118	16.84	-141.5	2.17	0.55	77.8	0.24	CJ2
0.040	40.35	-139.7	5.79	0.17	0.7	0.04	CJ1

3C 84 in which a relatively large value of  $D = 1.8$  is derived (Walker et al. 1994), suggesting a larger jet speed ( $v \sim 0.33c$ ) and a smaller viewing angle ( $\theta \sim 32^\circ$ ) for the value of the jet-counterjet brightness ratio,  $R$ , they measured. If CJ2, located around 20 mas from the core, is the counterpart of C2, then  $R \sim 4$ . This is consistent with the 8 GHz result discussed by Jones et al. (1996) for their beaming model.

The brightness temperature of the brightest component, Core1, is  $2.2 \times 10^{10}$  K, while Core2, the second most compact component in the core region, has a brightness temperature of  $9.1 \times 10^9$  K (table 1). Both the brightness temperatures are well below the inverse Compton limit. It is not yet clear how the free-free optical depth varies around the core at this resolution, but it is likely that the core region is substantially absorbed, and hence much brighter intrinsically. Assuming that the values derived by Tingay and Murphy (2001) are still applicable at this resolution, we can adopt an optical depth of 0.2 at 5 GHz and an intrinsic spectral index of 2.0 for the unresolved nuclear component, in which case the observed flux is expected to have been decreased to  $\sim 7\%$  of the original flux, indicating intrinsic brightness temperatures of  $\sim 3.1 \times 10^{11}$  K and  $1.3 \times 10^{11}$  K for Core1 and Core2, respectively. These values are still below the inverse Compton limit, but close to the limit calculated based on equipartition arguments (Readhead 1994).

Kellermann, Zensus, and Cohen (1997) measured a core size of 0.5 mas for Cen A with non-imaging visibility analysis of a few hr VLBA data taken at 43 GHz in 1994 April, fitting the visibilities with a circular Gaussian component. They also deduced the lower limit of the brightness temperature to be about  $10^{10}$  K for the peak visibility amplitude of about 5 Jy. The  $(u, v)$  distance range of our 5 GHz data is similar to the VLBA at 43 GHz, and we obtained the same rough source size and brightness temperature for our 5 GHz core component with a ten-times weaker flux. Although we measured similar values for the core brightness temperature for the 5 GHz core, if we consider an optical depth of 0.2 at 5 GHz and an intrinsic spectral index of 2.0, the estimated “equivalent” intrinsic flux density at 43 GHz for the 5 GHz core is about 8 times larger than the 43 GHz core flux density measured in 1994 April. This difference may be attributed to the significant variability of the core, which has been observed at high frequencies, such

as 22 GHz and 43 GHz (Botti, Abraham 1993).

### 3.2. Comparison with M 87

Marconi et al. (2001) have estimated the mass of the central black hole in Cen A to be  $2.0_{-1.4}^{+3.0} \times 10^8 M_\odot$ , from infrared spectra obtained at the Very Large Telescope. The Schwarzschild radii,  $r_s$ , for this mass is approximately 0.00002 pc, hence the spatial resolution of our observation 0.6 mas (0.012 pc at 4.3 Mpc distance) corresponds to  $600 r_s$ . Junor, Biretta, and Livio (1999) presented a 43 GHz VLBI image of the jet in M 87 (at a distance of 14.6 Mpc) on an angular scale of 0.12 mas, corresponding to a spatial scale of 0.009 mas, or  $30 r_s$  for the estimated black hole mass of  $3 \times 10^9 M_\odot$ . Their image shows a remarkably broad jet having an opening angle of  $\sim 60^\circ$  near the center, with strong collimation of the jet occurring at  $\sim 30$ – $100 r_s$  from the center, and collimation continuing out to  $\sim 1000 r_s$ . This seems to favor MHD disk wind models. In a seminal paper on this subject, Blandford and Payne (1982) demonstrated by simple analyses that ionized gas frozen onto magnetic field lines at the surface of the accretion disk will be unstable to outflow, if the angle of the field line to the vertical is  $\theta \geq 30^\circ$ , in which case the material will be flung outward along the field lines by the centrifugal force. The large opening angle of the jet seen at  $30 r_s$  distance from the center of M 87 seems to suggest that the jet originates from such a disk outflow (Junor et al. 1999, see also Meier et al. 2001 for a review). Because of the high linear scale resolution available to resolve the region around the black hole, Cen A is another ideal candidate for studies of the jet collimation mechanism.

Tingay, Preston, and Jauncey (2001) examined their Cen A data to see if they could measure a jet opening angle on a scale greater than their resolution ( $\sim 1000 r_s$ ); however, no evidence for a significant jet opening angle could be seen. In our image the jet appears to be significantly collinear from the core region to 60 mas (1 pc). If we assume that Core1 is the core, the jet opening angle of the first jet component C3 is  $\sim 12^\circ$  at a distance of 0.1 pc, or  $\sim 5000 r_s$  from the core. Interestingly, this angle and  $r_s$  distance are very similar to the results of the 5 GHz VSOP observations of M 87 included in Junor, Biretta, and Livio (1999, figure 3) as a part of the plot showing jet full

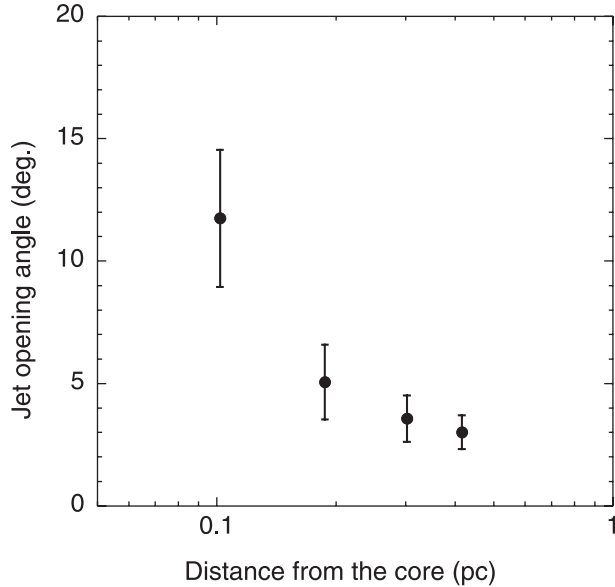


**Fig. 6.** Jet opening angle as a function of the distance from the core for Cen A. The error bars represent angles corresponding to one fourth of the beam size to indicate the uncertainties of measurement.

opening angle as function of distance from the core, although our distance of C3 from the core corresponds to 0.1 pc and their distance corresponds to 2 pc from the core. Figure 6 shows all of the measured jet opening angles for the components in the jet, excluding the counterjet and the core subcomponents. This result indicates that our observation marginally resolves the lower end of the collimation region in the Cen A jet. Future space VLBI missions, such as VSOP-2 at 22 GHz and

43 GHz (Hirabayashi et al. 2004), will probably be able to image the collimation region, within  $1000r_S$  from the center of Cen A, together with the accretion disk itself.

#### 4. Conclusion

We have presented a high-resolution VLBI image of the nearest radio galaxy, Cen A, observed at 4.9 GHz on 2000 August 6, which shows the subparsec-scale structure of the jet and the core on scales from 0.5 to approximately 50 milliarcsec from the core (0.01–1 pc projected linear distance). The elongated core region is resolved into several components of over 10 mas long. Model-fitting analyses have shown that the strongest peak is a compact component with a brightness temperature of  $2.2 \times 10^{10}$  K. The jet-to-counterjet brightness ratio is approximately 4 for a jet of around 20 mas from the core, consistent with previous observations at 2.3 and 8.4 GHz. Assuming the strongest component to be the core, the jet opening angle at  $\sim 5000r_S$  from the core is estimated to be  $\sim 12^\circ$  with collimation of the jet to  $\sim 3^\circ$ , continuing out to  $\sim 20000r_S$ , suggesting that collimation of the jet occurs inside this region, similar to that seen in M 87.

Part of this work was carried out at the Jet Propulsion Laboratory, California Institute of Technology, under contract to NASA, while S. H. held a National Research Council research associateship. We would like to thank P. Edwards for helpful comments. We gratefully acknowledge the VSOP Project, which is led by the Japanese Institute of Space and Astronautical Science in cooperation with many organizations and radio telescopes around the world.

#### References

- Blandford, R. D., & Payne, D. G. 1982, *MNRAS*, 199, 883  
 Botti, L. C. L., & Abraham, Z. 1993, *MNRAS*, 264, 807  
 Fujisawa, K., et al. 2000, *PASJ*, 52, 1021  
 Hardcastle, M. J., Worrall, D. M., Kraft, R. P., Forman, W. R., Jones, C., & Murray, S. S. 2003, *ApJ*, 593, 169  
 Hirabayashi, H., et al. 1998, *Science*, 281, 1825  
 Hirabayashi, H., et al. 2004, *Proc. SPIE*, 5487, 1646  
 Horiuchi, S., Meier, D. L., & Preston, R. A. 2002, *BAAS*, 34, 1245  
 Israel, F. P. 1998, *A&A Rev.*, 8, 237  
 Jones, D. L., et al. 1996, *ApJ*, 466, L63  
 Junor, W., Biretta, J. A., & Livio, M. 1999, *Nature*, 401, 891  
 Kellermann, K. I., Zensus, J. A., & Cohen, M. H. 1997, *ApJ*, 475, L93  
 Marconi, A., Capetti, A., Axon, D. J., Koekemoer, A., Macchetto, D., & Schreier, E. J. 2001, *ApJ*, 549, 915  
 Meier, D. L., Koide, S., & Uchida, Y. 2001, *Science*, 291, 84  
 Readhead, A. C. S. 1994, *ApJ*, 426, 51  
 Tingay, S. J., et al. 1998, *AJ*, 115, 960  
 Tingay, S. J., & Murphy, D. W. 2001, *ApJ*, 546, 210  
 Tingay, S. J., Preston, R. A., & Jauncey, D. L. 2001, *AJ*, 122, 1697  
 Walker, R. C., Romney, J. D., & Benson, J. M. 1994, *ApJ*, 430, L45